



HAL
open science

One-Sided Synthetic control charts for monitoring the Multivariate Coefficient of Variation

Thong Nguyen, Kim Phuc P Tran, Philippe Castagliola, Giovanni Celano, Salim Lardjane

► **To cite this version:**

Thong Nguyen, Kim Phuc P Tran, Philippe Castagliola, Giovanni Celano, Salim Lardjane. One-Sided Synthetic control charts for monitoring the Multivariate Coefficient of Variation. *Journal of Statistical Computation and Simulation*, 2019, 89 (10), pp.1841-1862. 10.1080/00949655.2019.1600694 . hal-01885435v2

HAL Id: hal-01885435

<https://hal.science/hal-01885435v2>

Submitted on 1 Apr 2019

HAL is a multi-disciplinary open access archive for the deposit and dissemination of scientific research documents, whether they are published or not. The documents may come from teaching and research institutions in France or abroad, or from public or private research centers.

L'archive ouverte pluridisciplinaire **HAL**, est destinée au dépôt et à la diffusion de documents scientifiques de niveau recherche, publiés ou non, émanant des établissements d'enseignement et de recherche français ou étrangers, des laboratoires publics ou privés.

One-Sided Synthetic control charts for monitoring the Multivariate Coefficient of Variation

Q. T. Nguyen^a, K. P. Tran^b, P. Castagliola^c, G. Celano^d and S. Lardjane^a

^aUniversité de Bretagne-Sud & LMBA UMR CNRS 6205, Vannes, France; ^bEcole Nationale Supérieure des Arts et Industries Textiles, GEMTEX Laboratory, BP 30329, 59056 Roubaix Cedex 1, France; ^cUniversité de Nantes & LS2N UMR CNRS 6004, Nantes, France;

^dUniversità di Catania, Catania, Italy

Abstract

Shewhart's type control charts for monitoring the Multivariate Coefficient of Variation (MCV) have recently been proposed in order to monitor the relative variability compared with the mean. These approaches are known to be rather slow in the detection of small or moderate process shifts. In this paper, in order to improve the detection efficiency, two one-sided Synthetic charts for the MCV are proposed. A Markov chain method is used to evaluate the statistical performance of the proposed charts. Furthermore, computational experiments reveal that the proposed control charts outperform the Shewhart MCV control chart in terms of the average run length to detect an out-of-control state. Finally, the implementation of the proposed chart is illustrated with an example using steel sleeves data.

KEYWORDS

Synthetic chart; Markov chain; Multivariate Coefficient of Variation; Steady-state

1. Introduction

Control charts are the most widely used Statistical Process Control tool. Under the usual assumptions, when implementing a control chart, the aim of quality practitioners is showing that the process position and/or scale are *independently* stable, to declare the in-control state for a process. However, in some processes, the location and scale are not independent of each other, that is, the population variance σ^2 is a function of the mean μ . In these situations, the process is assumed to be in the in-control state when a parameter defined as a function of both the mean and the variance is stable. When there is proportionality between μ and σ , monitoring the coefficient of variation CV is suggested: the coefficient of variation is defined as the ratio between the standard deviation and the mean. Monitoring the CV is of interest in those processes where the mean and the standard deviation may vary but their ratio is expected to be unchanged. Since the CV is a relative measure of dispersion, a control chart for the CV allows to detect the unexpected change in the ratio between μ and σ . Several control charts using different methods such as Run-sum [1], CUSUM [2], synthetic [3,4], EWMA [5,6] have been discussed in literature to monitor the coefficient of variation of a normal distribution [7–10].

In the past, attention to the need of monitoring the Multivariate CV (MCV) has been invoked in [11]. Today, with the huge increase of data availability from industrial processes, there is an outstanding interest on tools for online monitoring of multivariate

data. Therefore, considering the surveillance of the multivariate coefficient of variation is an issue worth of interest in SPM research. The first control chart aiming at monitoring the MCV was introduced by [12]: it is well known that Shewhart type control charts are easy to design and to interpret. Nevertheless, they are rather slow in the detection of small or moderate process shifts. For this reason several methods/strategies have been proposed in the SPC literature to overcome this weakness. For instance, the Run Sum control chart for the MCV was recently developed in [13]. In this paper, we propose a different approach for monitoring the MCV by using synthetic control charts.

Synthetic control charts have been widely used in literature to detect shifts in a process. The first introduction of the Synthetic \bar{X} chart to the field of SPC was in [14]; then, its properties and design strategies have been thoroughly investigated by many authors [15–21] for several monitoring statistics. Recently, [22] investigated the effect of estimated process parameters on the performance of the Synthetic chart using a Markov chain model. They have shown that the run length (RL) performance of the Synthetic chart is quite different in the *known* and in the *estimated* process parameters cases. However, as far as we know, the Synthetic control chart for monitoring the MCV has never been considered in the SPC literature. Therefore, the goal of this paper is to present and investigate the performance of two one-sided Synthetic MCV control charts. The decision to implement two one-sided synthetic MCV control charts instead of a single two-sided synthetic MCV control chart is motivated by the following reasons:

- The sample MCV distribution is *asymmetrical*: therefore, designing different control limits allows to get equal values of the in-control *ARL* for both the one-sided synthetic MCV control charts;
- there is more flexibility in the design of each one-sided synthetic MCV control chart: for example, if quality practitioners know that one direction of the out-of-control condition can occur more frequently than another, the control limit of each one-sided synthetic MCV control chart can be properly tuned to have a higher sensitivity vs. the most frequent shift direction.

The rest of the paper is organised as follows. A brief review of the distribution of the sample multivariate coefficient of variation is given in Section 2. The implementation of the two one-sided synthetic MCV control charts is described in Section 3. Section 4 discusses the performance of the synthetic MCV control charts. In Section 5, we illustrate a real-world example using our design. The concluding remarks are given in Section 6.

2. A brief review of the distribution of the sample multivariate coefficient of variation

In this Section, a brief overview of the distribution of the sample multivariate coefficient of variation is presented. Let us consider a random sample of size n , that is, $\mathbf{X}_1, \mathbf{X}_2, \dots, \mathbf{X}_n$ from a p -variate normal distribution with mean vector $\boldsymbol{\mu}$ and covariance matrix $\boldsymbol{\Sigma}$, i.e., $\mathbf{X}_i = (x_{i,1}, x_{i,2}, \dots, x_{i,p}) \sim N(\boldsymbol{\mu}, \boldsymbol{\Sigma})$, $i = 1, \dots, n$. According to [23], the MCV is defined as

$$\gamma = (\boldsymbol{\mu}^\top \boldsymbol{\Sigma}^{-1} \boldsymbol{\mu})^{-\frac{1}{2}}. \quad (1)$$

This definition is also used in [12] and [13]. Based on this definition of the MCV,

we can introduce the sample MCV and discuss its distribution. Let $\bar{\mathbf{X}}$ and \mathbf{S} be the sample mean vector and the sample variance-covariance matrix of $\mathbf{X}_1, \mathbf{X}_2, \dots, \mathbf{X}_n$, i.e.,

$$\bar{\mathbf{X}} = \frac{1}{n} \sum_{i=1}^n \mathbf{X}_i,$$

and

$$\mathbf{S} = \frac{1}{n-1} \sum_{i=1}^n (\mathbf{X}_i - \bar{\mathbf{X}})(\mathbf{X}_i - \bar{\mathbf{X}})^\top.$$

Then the sample multivariate coefficient of variation $\hat{\gamma}$ is defined in [12]

$$\hat{\gamma} = (\bar{\mathbf{X}}^\top \mathbf{S}^{-1} \bar{\mathbf{X}})^{-\frac{1}{2}}. \quad (2)$$

In [12], the cumulative distribution function (cdf) of $\hat{\gamma}$ is computed as

$$F_{\hat{\gamma}}(x|n, p, \gamma) = 1 - F_F\left(\frac{n(n-p)}{(n-1)px^2} | p, n-p, \frac{n}{\gamma^2}\right), \quad (3)$$

where $F_F(\cdot | p, n-p, \frac{n}{\gamma^2})$ is the non-central F cdf with p and $n-p$ degrees of freedom and non-centrality parameter $\frac{n}{\gamma^2} = n\boldsymbol{\mu}^\top \boldsymbol{\Sigma}^{-1} \boldsymbol{\mu}$. The probability density function (pdf) of $\hat{\gamma}$ can be easily obtained as

$$f_{\hat{\gamma}}(x|n, p, \gamma) = \frac{2n(n-p)}{(n-1)px^3} f_F\left(\frac{n(n-p)}{(n-1)px^2} | p, n-p, \frac{n}{\gamma^2}\right), \quad (4)$$

where $f_F(\cdot | p, n-p, \frac{n}{\gamma^2})$ is the pdf of non-central F distribution. In Figure 1, the pdf of $\hat{\gamma}$ is illustrated with $\gamma = 0.3$, $p = \{2, 3, 4\}$ and $n = \{5, 10, 15\}$. This example demonstrates the asymmetry of the $\hat{\gamma}$ distribution. In a similar way, [12] presented the inverse distribution function (idf) of $\hat{\gamma}$ as follows

$$F_{\hat{\gamma}}^{-1}(\alpha|n, p, \gamma) = \sqrt{\frac{n(n-p)}{(n-1)p} \left(\frac{1}{F_F^{-1}(1-\alpha | p, n-p, \frac{n}{\gamma^2})} \right)}, \quad (5)$$

where $F_F^{-1}(\cdot | p, n-p, \frac{n}{\gamma^2})$ is the inverse cdf of the non-central F distribution with p and $n-p$ degrees of freedom and non-centrality parameter $\frac{n}{\gamma^2}$.

3. Design and implementation of two one-sided the synthetic MCV control charts

In general, a synthetic control chart consists of two sub-charts: a Shewhart sub-chart and a conforming run length (CRL) sub-chart. The CRL is defined as the number of inspected samples between two consecutive nonconforming samples, inclusive of the nonconforming sample at the end [24]. Figure 2 illustrates how the CRL values are determined: in this example, we have $CRL_1 = 4$, $CRL_2 = 5$, and $CRL_3 = 3$. For the

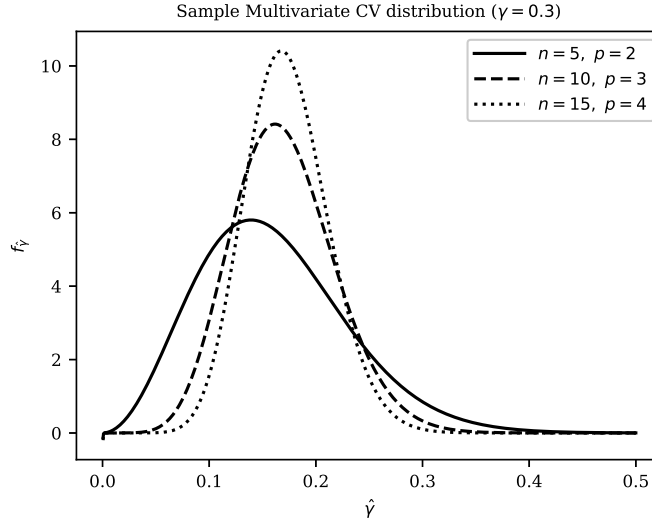


Figure 1. The pdf of $\hat{\gamma}$ for different values of parameters.

one-sided synthetic MCV control chart, the Shewhart sub-chart is defined as in [12]. Therefore, a j -th sample is declared as nonconforming if $\hat{\gamma}_j$, $j = 1, 2, \dots$, falls beyond the selected control limits of the one-sided Shewhart MCV sub-chart. As mentioned, in this study, two one-sided synthetic control charts for monitoring the MCV are designed: a lower-sided synthetic MCV control chart and an upper-sided synthetic MCV control chart. For the purpose of distinguishing the two control charts, the superscript "–" will be used for the control limits of sub-charts running the lower-sided control chart, while the superscript "+" will be used for the control limits of sub-charts running the upper-sided control chart. The operation of the one-sided synthetic MCV control charts can be summarized as follows:

Step 1 Fix the sample size n . For the synthetic lower-sided (upper-sided) MCV chart, determine the control limit H^- (H^+) of the CRL sub-chart and the lower (upper) control limit LCL^- (UCL^+) of the Shewhart MCV sub-chart. The synthetic lower-sided (upper-sided) MCV chart is run to detect a decreasing (increasing) shift in $\hat{\gamma}_j$ with a single Lower (Upper) Control Limit LCL^- (UCL^+), i.e. $UCL^- = +\infty$ ($LCL^+ = 0$).

Without any misunderstanding, the lower control limit LCL^- of the one-sided lower Shewhart MCV sub-chart and the upper control limit UCL^+ of the one-sided upper Shewhart MCV sub-chart can be simply written as LCL and UCL , respectively.

Step 2 At each sampling point $j = 1, 2, \dots$, take a sample of size n from the process and evaluate the sample MCV $\hat{\gamma}_j$ as in (2).

Step 3 If $\hat{\gamma}_j > LCL$ (respectively, $\hat{\gamma}_j < UCL$ in case of the upper-sided synthetic MCV control chart), this sample is considered as conforming in the CRL sub-chart: the process is considered to be in-control and the control flow goes back to step 2 to take the next sample. Otherwise, the sample is nonconforming and the control flow goes to the next step.

Step 4 If $CRL > H^-$ (respectively, $CRL > H^+$ in case of the upper-sided one-sided lower Shewhart MCV sub-chart) the process is deemed to be in-control and the

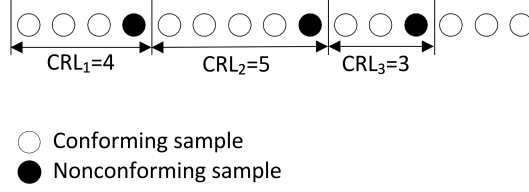


Figure 2. The conforming run length (CRL).

control flow moves back to step 2. Otherwise, the process is declared to be in the out-of-control state and the control flow advances to the next step.

Step 5 Signal an out-of-control status to indicate a process shift. Find and remove potential assignable cause(s). Then move back to Step 2.

We assume that the occurrence of an out-of-control condition shifts the in-control MCV, denoted by γ_0 , to the out-of-control MCV, defined as $\gamma_1 = \tau\gamma_0$, where $\tau > 0$ is the shift size. Values of $\tau \in (0, 1)$ correspond to a decrease of the in-control MCV γ_0 , while values of $\tau > 1$ correspond to an increase of the in-control MCV γ_0 . In order to obtain the run length properties of the lower-sided Synthetic MCV control chart, similarly to [15], we use a Markov chain where the $(H^- + 2, H^- + 2)$ transition probability matrix \mathbf{P} is equal to

$$\mathbf{P} = \begin{pmatrix} \mathbf{Q} & \mathbf{r} \\ \mathbf{0}^\top & 1 \end{pmatrix} = \left(\begin{array}{cccccc|c} 1-\theta & \theta & 0 & \cdots & \cdots & 0 & 0 \\ 0 & 0 & 1-\theta & \ddots & & 0 & \theta \\ \vdots & & \ddots & \ddots & \ddots & \vdots & \vdots \\ \vdots & & & \ddots & 1-\theta & 0 & \vdots \\ 0 & \cdots & \cdots & \cdots & 0 & 1-\theta & \theta \\ 1-\theta & 0 & \cdots & \cdots & \cdots & 0 & \theta \\ \hline 0 & \cdots & \cdots & \cdots & \cdots & 0 & 1 \end{array} \right), \quad (6)$$

where $\mathbf{0}^\top = (0, 0, \dots, 0)$ is a $(1, H^- + 1)$ row vector, \mathbf{Q} is a $(H^- + 1, H^- + 1)$ transition probability matrix for the transient states, the $(H^- + 1, 1)$ column vector \mathbf{r} satisfies $\mathbf{r} = \mathbf{1} - \mathbf{Q}\mathbf{1}$ with $\mathbf{1} = (1, 1, \dots, 1)^\top$ and $\theta = P(\gamma_j \leq LCL)$ is the probability of a nonconforming sample on the MCV sub-chart. In case of the upper-sided synthetic MCV control chart, H^- is replaced by H^+ and $\theta = P(\gamma_j \geq UCL)$.

- For the lower-sided control chart

$$\theta = F_{\hat{\gamma}}(LCL|n, p, \gamma_1).$$

- For the upper-sided control chart

$$\theta = 1 - F_{\hat{\gamma}}(UCL|n, p, \gamma_1),$$

Since the calculation in case of the lower-sided control chart is similar to the one of an upper-sided control chart, in the next discussion we only focus on the synthetic lower-sided MCV control chart. The differences with the upper-sided control chart will be discussed when it is required. The corresponding $(H^- + 1, 1)$ vector \mathbf{q} of the initial prob-

abilities associated with the $H^- + 1$ transient states is equal to $\mathbf{q} = (q_1, \dots, q_{H^-+1})^\top$. As proposed by [25] and [26], the mean of the run length (ARL) and the standard-deviation ($SDRL$) of the run length of the synthetic MCV control chart are computed as

$$ARL_{ZS} = \nu_1, \quad (7)$$

$$SDRL_{ZS} = \sqrt{\nu_2 - \nu_1^2 + \nu_1}, \quad (8)$$

with

$$\nu_1 = \mathbf{q}^\top (\mathbf{I} - \mathbf{Q})^{-1} \mathbf{1}, \quad (9)$$

$$\nu_2 = 2\mathbf{q}^\top (\mathbf{I} - \mathbf{Q})^{-2} \mathbf{Q} \mathbf{1}, \quad (10)$$

and $\mathbf{q} = (0, 1, 0, \dots, 0)^\top$, i.e. the initial state is the second one, as suggested in [22]. With this vector q of initial probabilities, we are able to obtain the zero-state performance of the synthetic MCV control chart. The subscript "ZS" stands for zero-state condition.

It is important to note that, if the process is running for some time in the in-control condition, it will reach quite rapidly the steady-state mode. In order to study the long term properties of the synthetic MCV control chart, it is also appropriate to investigate the steady-state ARL . Using the Markov Chain approach, the *cyclical* steady-state mean (ARL_{SS}) and the standard-deviation ($SDRL_{SS}$) of the run length of the Synthetic MCV control chart are found as follows

$$ARL_{SS} = \nu_{s1}, \quad (11)$$

$$SDRL_{SS} = \sqrt{\nu_{s2} - \nu_{s1}^2 + \nu_{s1}} \quad (12)$$

with

$$\nu_{s1} = \boldsymbol{\psi}^\top (\mathbf{I} - \mathbf{Q})^{-1} \mathbf{1}, \quad (13)$$

$$\nu_{s2} = 2\boldsymbol{\psi}^\top (\mathbf{I} - \mathbf{Q})^{-2} \mathbf{Q} \mathbf{1}, \quad (14)$$

where the vector $\boldsymbol{\psi}$ is the *cyclical* steady state distribution. Following [27], we conclude that the *cyclical* steady-state vector is given by $\boldsymbol{\psi} = \frac{(\mathbf{I} - \mathbf{Q}^\top)^{-1} \mathbf{q}}{\mathbf{1}^\top (\mathbf{I} - \mathbf{Q}^\top)^{-1} \mathbf{q}}$, where \mathbf{q} is the $(H^- + 1, 1)$ vector, $\mathbf{q} = (0, 1, 0, \dots, 0)^\top$.

The statistical design of the synthetic lower-sided MCV control control chart is a nonlinear optimization problem aimed at selecting the optimal parameters H^{-*} such that

$$(H^{-*}, LCL^*) = \arg \min_{(H^-, LCL)} ARL(n, p, H^-, LCL, \gamma_0, \tau), \quad (15)$$

subject to

$$ARL(n, p, H^-, LCL, \gamma_0, \tau = 1) = ARL_0, \quad (16)$$

where $ARL(n, p, H^-, LCL, \gamma_0, \tau)$ is either the zero-state ARL_{ZS} or the *cyclical* steady state ARL_{SS} of the synthetic lower-sided MCV control chart; ARL_0 is the nominal

“in-control” (zero-state or *cyclical* steady state) *ARL*. The optimization procedure can be summarized as follows:

- Step 1** Set n, p, γ_0, τ and ARL_0 . Set $ARL_{opt} = +\infty$;
- Step 2** Initialize $H^- = 1$;
- Step 3** Compute *LCL* through constraint (16);
- Step 4** Compute *ARL* from the current design solution H^- by using either (7) or (11);
- Step 5** If $ARL < ARL_{opt}$, then $ARL_{opt} = ARL$ and $H^{-*} = H^-, LCL^* = LCL$. Set $H^- = H^- + 1$ and go back to Step 3. Otherwise, go to Step 6;
- Step 6** Take the current solution (H^{-*}, LCL^*) as the optimal set of design parameters for the synthetic MCV control chart.

Similar to [2], the optimal *LCL* is found numerically by means of a non-linear equation solver developed in the Matlab software environment. For the case of an upper-sided control chart, H^- is replaced by H^+ and *LCL* by *UCL*. Similarly, the optimization problem is as follows:

$$(H^{+*}, UCL^*) = \arg \min_{(H^+, UCL)} ARL(n, p, H^+, UCL, \gamma_0, \tau), \quad (17)$$

subject to

$$ARL(n, p, H^+, UCL, \gamma_0, \tau = 1) = ARL_0, \quad (18)$$

4. Statistical Performance Study

4.1. Performance with known shift size

In this Section, we will use the *ARL*, *SDRL* to evaluate the performance of the synthetic MCV charts. When the process is in-control, the target *ARL* is denoted by ARL_0 : here, we set $ARL_0 = 370.4$. For the lower side synthetic MCV control chart, the optimal design parameters (H^{-*}, LCL^*) and zero-state *ARL* are shown in Table 2 for different combinations of $n = \{5, 10, 15\}$, $p = \{2, 3, 4\}$, $\gamma_0 = \{0.1, 0.2, 0.3, 0.4, 0.5\}$ and $\tau = \{0.5, 0.75, 0.9\}$. Table 3 illustrates the optimal design parameters (H^{+*}, UCL^*) and the zero-state the *ARL* for the upper-sided synthetic MCV control chart with the same combinations of n, p, γ_0 as in Table 2 but $\tau = \{1.1, 1.25, 1.5\}$. In case of steady-state condition, the same results are presented in Table 4 and Table 5.

From Table 2-5, the H^{-*}, H^{+*}, ARL and *SDRL* values for both the lower-sided and the upper-sided control charts are larger when τ is close to 1. For example, by referring to Table 2 under the zero-state condition, with $p = 2, n = 10, \gamma_0 = 0.1$ and $\tau = 0.5$, the values of ARL_{ZS} and $SDRL_{ZS}$ are 1.5 and 1.1, respectively; while ARL_{ZS} and $SDRL_{ZS}$ are 105.4 and 128.2, respectively when $\tau = 0.9$. This was expected, since the shift is smaller when τ is close to 1. Similar behavior is observed with regards to the sample size n : the larger is the sample size, the smaller is the number of samples needed to detect an out-of-control situation in average; also the *SDRL* is smaller. For instance, as shown in Table 4 under the steady-state condition with $\gamma_0 = 0.1, \tau = 0.75, p = 4$; the ARL_{SS} and $SDRL_{SS}$ values are 212.5 and 211.8, respectively when $n = 5$, with $n = 10$, these values are $ARL_{SS} = 32.9$ and $SDRL_{SS} = 31.7$, respectively. This improved performance with n is more significant for larger values of p . Therefore, a larger sample size is recommended when more variables are monitored.

It is also observed that the ARL and $SDRL$ values are larger for the lower-sided control chart compared to the upper-sided control chart. On the contrary, the H^{-*} values for the lower-sided control chart are smaller than the H^{+*} values for the upper-sided control chart. For example, in Tables 2-3, with $p = 2, n = 10$ and $\gamma_0 = 0.1$, ARL_{ZS} , $SDRL_{ZS}$ and H^{-*} of the lower-sided control chart are 105.4, 128.2 and 11, respectively, when $\tau = 0.9$, while ARL_{ZS} , $SDRL_{ZS}$ and H^{+*} of the upper-sided control chart are 44.1, 57.4 and 31, respectively, when $\tau = 1.1$. In the other words, it is easier to detect the upward shift in MCV than the downward shift. The different behavior between the lower-sided control chart and the upper-sided control chart is due to the asymmetric of the distribution of the MCV, see Figure 1. In practice, the detection of an upward shift is usually more important, as an upward shift indicates an increase of relative variation with regard to the mean.

Both the optimal values H^{+*} and H^{-*} are smaller when the shift is large. In addition, when the sample size n increases, we observed that, the values of H^{+*} decreases in both zero-state and steady-state conditions. On the other hand, the values of H^{-*} increase in both conditions when n increases. The design optimization algorithm runs to minimize the average run length: due to the asymmetry of the distribution of the MCV, the trends of H^{+*} and H^{-*} are different. **Moreover, it is observed that, in some cases, the values H are larger than the ARL values. For instance, at the end of Table 3, with $p = 4, n = 5, \tau = 1.5$, the values of H^{+*} and ARL_{ZS} are 26 and 19.5, respectively. In fact, as illustrated in Figure 3, the decrease of ARL with respect to H is insignificant when the ARL is close to the minimum.**

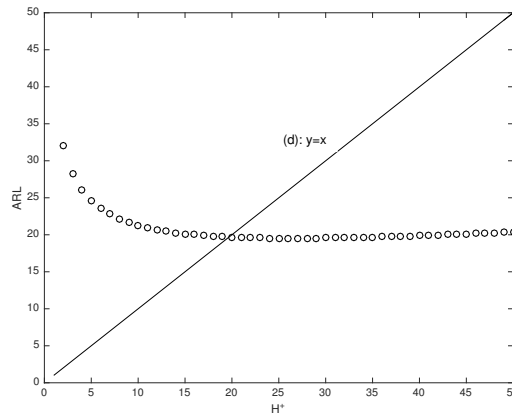


Figure 3. The variation of ARL with respect to H .

For a larger value of γ_0 , a larger LCL^* for the lower-sided control chart is adopted; the value of UCL^* is also larger for the upper side chart. When the sample size n increases, LCL^* also increases for the lower side control chart, while UCL^* does not significantly change. It is also observed that the higher in-control MCV γ_0 slightly increases the average number of samples needed to detect a process shift.

PLEASE INSERT TABLES 2, 3, 4, 5 HERE

The performance comparison between the ARL values of the one-sided Synthetic MCV control charts and the ARL values of the one-sided Shewhart MCV control charts proposed in [12] is provided in Table 6. The The performance comparison has

been undertaken by defining the following index Δ_E

$$\Delta_E = \frac{ARL_{SH} - ARL_{syn}}{ARL_{SH}} \times 100, \quad (19)$$

where ARL_{SH} is the average run length value for the Shewhart MCV control chart, while ARL_{syn} is the average run length value for the synthetic MCV control chart. If $\Delta_E > 0$, then the Synthetic MCV charts outperform the Shewhart MCV charts; if $\Delta_E < 0$, then the Shewhart MCV charts outperform the Synthetic MCV charts. The obtained results presented in Tables 6, rounded to the nearest integer, show that the Synthetic MCV charts outperform the Shewhart MCV charts for both the lower-sided and the upper-sided control charts. The Synthetic MCV charts are significantly better than the Shewhart MCV charts when the shift size is large, i.e. $|\tau - 1|$ is large.

PLEASE INSERT TABLE 6 HERE

4.2. Performance with unknown shift size

We already know that the synthetic MCV control charts can be optimally designed in terms of ARL for quickly detecting anticipated shift sizes. However, in practice, the shift size τ to the out-of-control condition cannot be predicted with sufficient precision. In order to overcome this problem, the uncertainty related to the shift size prediction can be tackled by considering τ as a random variable and selecting a statistical distribution to model it. Several potential statistical distributions have been considered in the literature, see [28]. If the quality practitioner wants to get an optimal design of a control chart with respect to a range of shifts sizes $\Omega = [a, b]$, without any preference for a specific size, then the uniform distribution can be selected to give an equal weight to each shift size included within the interval Ω , see [28]. Therefore, in the second step of our numerical analysis, we have computed *new* optimal couples (H^{-*}, LCL^*) or (H^{+*}, UCL^*) , such that

- For the lower-sided control chart:

$$(H^{-*}, LCL^*) = \arg \min_{(H^-, LCL)} EARL(n, p, H^-, LCL, \gamma_0, \tau)$$

subject to the constraint

$$EARL(n, p, H^-, UCL^-, \gamma_0, \tau = 1) \quad (20)$$

$$= ARL(n, p, H^-, UCL^-, \gamma_0, \tau = 1) = ARL_0, \quad (21)$$

- For the upper-sided control chart:

$$(H^{+*}, UCL^*) = \arg \min_{(H^+, UCL)} EARL(n, p, H^+, UCL, \gamma_0, \tau)$$

subject to the constraint

$$EARL(n, p, H^+, UCL, \gamma_0, \tau = 1) \quad (22)$$

$$= ARL(n, p, H^+, UCL, \gamma_0, \tau = 1) = ARL_0, \quad (23)$$

where $EARL$ (Expected Average Run Length) is equal to

$$EARL = \int_{\Omega} ARL \times f_{\tau}(\tau) d\tau, \quad (24)$$

with $f_{\tau}(\tau) = \frac{1}{b-a}$ for $\tau \in \Omega = [a, b]$ and ARL is defined as in (7). The *new* optimal couples ((H^{-*}, LCL^*) and (H^{+*}, UCL^*)) and the values of $EARL$ are presented in Tables 7-8 for $\Omega = [0.5, 1)$ (decreasing case, denoted by (D)) and $\Omega = (1, 2]$ (increasing case, denoted by (I)). Table 7 presents the zero-state performance, while Table 8 presents the steady state performance.

Similar to the known shift case, $EARL$ values are larger for the lower-sided chart, if compared to the upper-sided chart. While the H^{-*} values are small compared to the H^{+*} values. Detecting the upward shift in MCV is easier than the downward shift. As expected, the control chart sensitivity improves with the sample size. Increasing the sample size n also leads to a tighter in-control interval on the chart. It is also observed that the higher in-control MCV γ_0 slightly increases the $EARL$ values. With regards to the number of monitored variables, the values of $EARL$ increase with p . Therefore, a larger sample size is always recommended when we have more correlated variables.

PLEASE INSERT TABLE 7, 8 HERE

The performance comparison between the ARL values of the Synthetic MCV control charts with the ARL values for the Shewhart MCV control charts (on both upper-sided and lower-sided cases) is also conducted. The comparison indices computed by (19) are provided in Table 9. The results show that the Synthetic MCV charts always outperform the Shewhart MCV chart in the unknown shift case. Moreover, the Synthetic MCV control charts perform much better when more samples are taken.

PLEASE INSERT TABLE 9 HERE

In addition, we also make a direct comparison of ARL values with the run sum MCV control chart developed by [13]. The experiments in [13] are only conducted with $\gamma_0 = \{0.1, 0.3, 0.5\}$, $p = \{2, 3\}$ and $n = \{5, 10\}$, see Tables 1-4 in [13]. The value of ARL_0 in this comparison is 370. Under the zero-state condition, as shown in Table 10, the upper-sided synthetic control chart is able to detect sooner the upward shift in MCV. For example, with $\gamma_0 = 0.1, \tau = 1.25, p = 3$ and $n = 10$, the results of ARL are 9.1 and 11.8 for the synthetic upper-sided MCV and run sum MCV control charts, respectively. However, the run sum MCV control chart performs better than the synthetic lower-sided MCV control chart in detecting the downward shift. Similarly, when the shift size is unknown, the synthetic MCV control charts are faster than the run sum MCV control chart in detecting upward shifts.

PLEASE INSERT TABLE 10 HERE

Finally, we compare the performance of the synthetic MCV control charts with the very recent adaptive MCV control charts designed in [29]. In order to make a fair comparison, only the upward control charts are investigated and the parameters used in [29] are $\gamma_0 = \{0.1, 0.3, 0.5\}$, $p = \{2, 3\}$, $\tau = \{1.25, 1.5\}$ and $n = \{5, 10\}$, see Tables 3-4 in [29]. And a Synthetic chart is considered as a fixed sampling interval control chart with $h = 1$. As presented in Table 11, the variable sample size and sampling interval (VSSI) and variable sample size (VSS) MCV control charts outperform the Synthetic MCV control chart. On the other hand, the Synthetic MCV control chart gives a better performance than the variable sampling interval (VSI) control chart

in most cases. However, it should be noted that, in [29], the results are only given under the steady-state condition. Moreover, the Synthetic MCV charts work well under the zero-state condition. Therefore, we cannot draw a general conclusions about the performance difference.

PLEASE INSERT TABLE 11 HERE

5. Illustrative example

In this Section, we discuss the implementation of the upper-sided and the lower-sided control charts. The context of the example presented here is similar to the one introduced in [13]. As discussed in [13], the data are obtained from a company, for which the quality characteristics are the inner diameters A and B, whose measurements are presented by (X_1) and (X_2) . From phase I, the value of MCV has been estimated, i.e. $\hat{\gamma}_0 = 0.089115$. The data collected during the phase II process with sample size $n = 5$ are shown in Table 1.

Sample number i	$\bar{X}_{1,i}$	$\bar{X}_{2,i}$	$S_{1,i}^2$	$S_{2,i}^2$	$S_{12,i}$	$\hat{\gamma}_i$
1	7.781	1.592	1.164	0.734	0.35645	0.113710
2	7.385	1.804	1.006	1.667	0.96049	0.104890
3	7.988	2.260	0.762	0.359	0.17373	0.108870
4	8.189	2.100	1.885	0.470	0.13026	0.156790
5	7.436	2.061	1.404	0.519	0.08280	0.139290
6	6.746	2.289	0.846	0.811	0.43835	0.133240
7	7.356	1.917	0.197	2.587	0.01597	0.059996
8	8.492	1.845	1.460	1.746	1.42051	0.055093
9	7.272	1.580	1.353	0.345	0.27988	0.117710
10	7.585	1.568	1.098	0.788	0.41252	0.109610
11	7.734	1.709	0.952	0.228	0.11462	0.102440
12	8.160	1.498	1.598	1.178	1.00757	0.122950
13	7.102	2.661	1.508	0.945	0.73607	0.101260
14	8.392	1.883	0.536	0.706	0.23234	0.085637
15	7.592	2.531	0.256	0.563	0.24827	0.043489
16	8.141	2.093	0.394	0.603	0.25584	0.072202
17	7.883	2.490	1.321	1.179	0.65037	0.142430
18	7.886	2.877	0.883	1.431	0.22524	0.106680
19	7.830	1.008	0.878	0.558	0.14223	0.112090
20	8.196	1.482	0.791	0.220	0.13724	0.088460

Table 1. Illustrative example of Phase II dataset.

In this case, the upper-sided and the lower-sided control charts, which are designed for a quick detection of a 25% increasing shift (i.e., $\tau = 1.25$) and a 25% decreasing shift (i.e., $\tau = 0.75$) in the MCV, are implemented simultaneously. Based on the optimization procedure in Sec. 3 with $ARL_0 = 370.4$, we obtain $(H^{+*} = 22, UCL^* = 0.1487)$ and $(H^{-*} = 3, LCL^* = 0.0221)$ for the upper-sided and the lower-sided control charts respectively.

The corresponding values $\hat{\gamma}_i$ are presented in the rightmost column of Table 1 and plotted in Figures 4 and 5, respectively. At sample #4, a point is plotted above $UCL^* = 0.1487$ and a conforming run length $CRL_1 = 4 < H^{+*} = 22$ is recorded. Therefore,

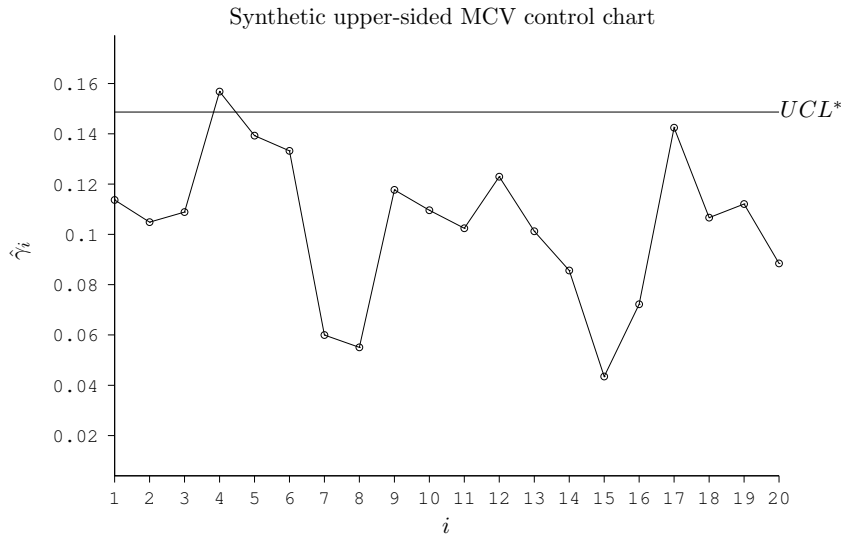


Figure 4. Synthetic upper-sided control chart corresponding to Phase II data set in Table 1.

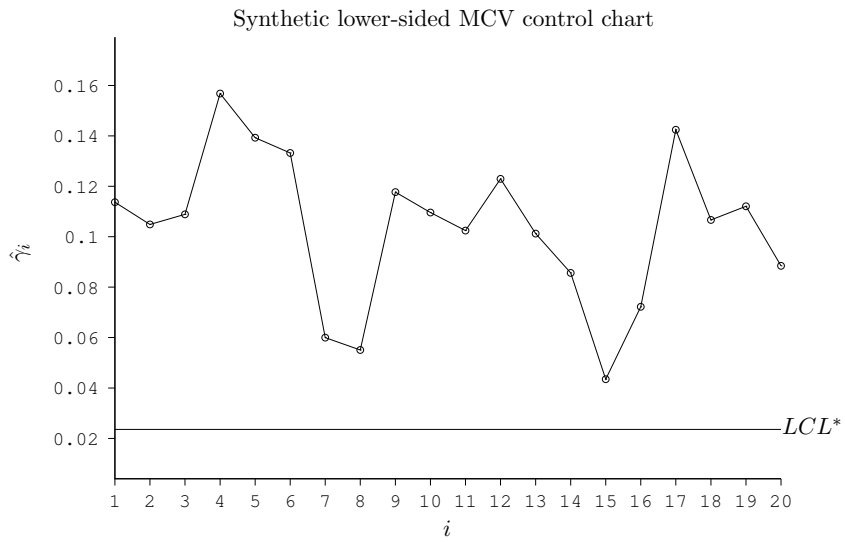


Figure 5. Synthetic lower-sided control chart corresponding to Phase II data set in Table 1.

the upper-sided control chart triggers an alarm signaling at sample #4. Conversely, the lower-sided control chart does not detect any out-of-control signal.

6. Concluding remarks

Monitoring the multivariate coefficient of variation is recently receiving growing attention in the context of SPC. In this study, we proposed two one-sided synthetic control charts for monitoring the MCV: synthetic lower-sided and synthetic upper-sided MCV control charts. By combining the Shewhart chart with a conforming run length (*CRL*) chart, the performance of the control charts are significantly improved. The paper presents both zero-state and steady-state conditions for the control charts. For both fixed values of the shift size τ and unknown shift size, several tables presenting the optimal design parameters and out-of-control *ARL* corresponding to different values of the in-control MCV γ_0 have been discussed. In this paper we also illustrate a practical example from a manufacturing process.

The synthetic control charts for monitoring MCV are simple to implement, yet effectively enhance the detection ability. A comparison with the one-sided Shewhart MCV control charts demonstrated the clear outperformance of the synthetic one-sided MCV control charts. The synthetic upper-sided MCV chart also performs better the run sum MCV chart. The future research about monitoring the MCV can be extended to adaptive schemes with variable parameters and the design of EWMA and CUSUM control charts.

References

- [1] Teoh W, Khoo M, Castagliola P, et al. Run-sum control charts for monitoring the coefficient of variation. *European Journal of Operational Research*. 2017;257(1):144–158.
- [2] Tran P, Tran KP. The Efficiency of CUSUM schemes for monitoring the Coefficient of Variation. *Applied Stochastic Models in Business and Industry*. 2016;32(6):870–881.
- [3] Calzada ME, Scariano SM. A synthetic control chart for the coefficient of variation. *Journal of Statistical Computation and Simulation*. 2013;83(5):853–867.
- [4] Tran KP, Nguyen HD, Nguyen QT, et al. One-sided synthetic control charts for monitoring the coefficient of variation with measurement errors. In: 2018 IEEE International Conference on Industrial Engineering and Engineering Management (IEEM); Dec; 2018. p. 1667–1671.
- [5] Zhang J, Li Z, Chen B, et al. A new exponentially weighted moving average control chart for monitoring the coefficient of variation. *Computers & Industrial Engineering*. 2014; 78:205–212.
- [6] Castagliola P, Celano G, Psarakis S. Monitoring the coefficient of variation using EWMA charts. *Journal of Quality Technology*. 2011;43(3):249–265.
- [7] Khaw KW, Khoo MB, Yeong WC, et al. Monitoring the coefficient of variation using a variable sample size and sampling interval control chart. *Communications in Statistics-Simulation and Computation*. 2017;46(7):5772–5794.
- [8] Yeong WC, Khoo MB, Lim SL, et al. A direct procedure for monitoring the coefficient of variation using a variable sample size scheme. *Communications in Statistics-Simulation and Computation*. 2017;46(6):4210–4225.
- [9] You HW, Khoo MB, Castagliola P, et al. Monitoring the coefficient of variation using the side sensitive group runs chart. *Quality and Reliability Engineering International*. 2016; 32(5):1913–1927.

- [10] Kang CW, Lee MS, Seong YJ, et al. A control chart for the coefficient of variation. *Journal of quality technology*. 2007;39(2):151–158.
- [11] Aerts S, Haesbroeck G, Ruwet C. Multivariate coefficients of variation: Comparison and influence functions. *Journal of Multivariate Analysis*. 2015;142:183–198.
- [12] Yeong W, Khoo MBC, LTeoh W, et al. A control chart for the multivariate coefficient of variation. *Quality and Reliability Engineering International*. 2016;32(3):1213–1225.
- [13] Lim AJ, Khoo MB, Teoh W, et al. Run sum chart for monitoring multivariate coefficient of variation. *Computers & Industrial Engineering*. 2017;109:84–95.
- [14] Wu Z, Spedding T. A Synthetic Control Chart for Detecting Small Shifts in the Process Mean. *Journal of Quality Technology*. 2000;32(1):32–38.
- [15] Davis RB, Woodall WH. Evaluating and improving the synthetic control chart. *Journal of Quality Technology*. 2002;34(2):200.
- [16] Chen F, Huang H. A Synthetic Control Chart for Monitoring Process Dispersion with Sample Range. *International Journal of Advanced Manufacturing Technology*. 2005;26(7-8):842–851.
- [17] Huang H, Chen F. A Synthetic Control Chart for Monitoring Process Dispersion with Sample Standard Deviation. *Computers & Industrial Engineering*. 2005;49(2):221–240.
- [18] Costa A, Rahim M. A Synthetic Control Chart for Monitoring the Process Mean and Variance. *Journal of Quality in Maintenance Engineering*. 2006;12(1):81–88.
- [19] Costa A, de Magalhaes M, Epprecht E. Monitoring the Process Mean and Variance Using a Synthetic Chart with Two-stage Testing. *International Journal of Production Research*. 2009;47(18):5067–5086.
- [20] Wu Z, Ou Y, Castagliola P, et al. A Combined Synthetic&X Chart for Monitoring the Process Mean. *International Journal of Production Research*. 2010;48(24):7423–7436.
- [21] Khoo M, Lee H, Wu Z, et al. A Synthetic Double Sampling Control Chart for the Process Mean. *IIE Transactions*. 2011;43(1):23–38.
- [22] Zhang Y, Castagliola P, Wu Z, et al. The synthetic [xbar] chart with estimated parameters. *IIE Transactions*. 2011;43(9):676–687.
- [23] Nikulin M, Voinov V. Unbiased estimators and their applications. In: *International encyclopedia of statistical science*. Springer; 2011. p. 1619–1621.
- [24] You H, Khoo MB, Castagliola P, et al. Side sensitive group runs \bar{x} chart with estimated process parameters. *Computational Statistics*. 2015;30(4):1245–1278.
- [25] Neuts M. *Matrix-Geometric Solutions in Stochastic Models: an Algorithmic Approach*. Baltimore, MD: Johns Hopkins University Press; 1981.
- [26] Latouche G, Ramaswami V. *Introduction to Matrix Analytic Methods in Stochastic Modelling*. Philadelphia, PA: Series on Statistics and Applied Probability. SIAM; 1999.
- [27] Darroch J, Seneta E. On quasi-stationary distributions in absorbing discrete-time finite markov chains. *Journal of Applied Probability*. 1965;2(1):88–100.
- [28] Celano G, Castagliola P, Nenes G, et al. Performance of t Control Charts in Short Runs with Unknown Shift Sizes. *Computers & Industrial Engineering*. 2013;64:56–68.
- [29] Khaw KW, Khoo MB, Castagliola P, et al. New adaptive control charts for monitoring the multivariate coefficient of variation. *Computers & Industrial Engineering*. 2018;126:595–610.

p	τ	$n = 5$				$n = 10$				$n = 15$			
		H^{-*}	LCL^*	ARL_{ZS}	$SDRL_{ZS}$	H^{-*}	LCL^*	ARL_{ZS}	$SDRL_{ZS}$	H^{-*}	LCL^*	ARL_{ZS}	$SDRL_{ZS}$
$\gamma_0 = 0.1$													
2	0.50	2	0.0266	10.6	12.8	2	0.0523	1.5	1.1	2	0.0624	1.1	0.3
2	0.75	3	0.0248	77.3	88.7	6	0.0480	16.3	20.6	5	0.0593	6.9	8.4
2	0.90	3	0.0248	206.6	227.4	11	0.0459	105.4	128.2	12	0.0566	66.0	82.7
3	0.50	1	0.0163	27.3	30.8	2	0.0463	1.8	1.6	2	0.0587	1.1	0.4
3	0.75	1	0.0163	122.7	131.9	6	0.0422	20.7	26.1	5	0.0556	7.9	9.8
3	0.90	1	0.0163	246.6	260.4	10	0.0404	118.0	141.9	12	0.0529	71.7	89.5
4	0.50	1	0.0032	93.4	101.2	2	0.0400	2.3	2.3	2	0.0548	1.1	0.5
4	0.75	1	0.0032	209.1	221.7	6	0.0360	27.0	33.8	5	0.0517	9.2	11.5
4	0.90	1	0.0032	300.5	315.9	9	0.0347	133.4	158.3	12	0.0491	78.3	97.3
$\gamma_0 = 0.2$													
2	0.50	2	0.0528	10.9	13.2	2	0.1037	1.5	1.2	2	0.1240	1.1	0.3
2	0.75	3	0.0492	78.8	90.4	6	0.0952	17.1	21.6	5	0.1177	7.2	8.9
2	0.90	3	0.0492	208.5	229.4	11	0.0910	108.0	131.3	13	0.1119	68.4	85.9
3	0.50	1	0.0323	27.9	31.5	2	0.0918	1.8	1.6	2	0.1164	1.1	0.4
3	0.75	1	0.0323	124.5	133.8	6	0.0836	21.6	27.2	5	0.1103	8.3	10.4
3	0.90	1	0.0323	248.2	262.1	10	0.0801	120.7	145.0	12	0.1050	74.2	92.4
4	0.50	1	0.0064	94.7	102.6	2	0.0792	2.4	2.4	2	0.1086	1.2	0.5
4	0.75	1	0.0064	210.7	223.4	6	0.0712	28.1	35.2	5	0.1025	9.7	12.2
4	0.90	1	0.0064	301.5	316.9	9	0.0686	136.1	161.5	12	0.0973	80.9	100.3
$\gamma_0 = 0.3$													
2	0.50	2	0.0781	11.4	13.8	2	0.1536	1.6	1.3	2	0.1838	1.1	0.4
2	0.75	3	0.0729	81.4	93.2	6	0.1409	18.3	23.2	5	0.1744	7.9	9.8
2	0.90	3	0.0729	211.5	232.6	11	0.1346	112.2	136.0	13	0.1656	72.1	90.3
3	0.50	1	0.0478	29.1	32.7	2	0.1358	1.9	1.8	2	0.1724	1.1	0.4
3	0.75	1	0.0478	127.5	136.9	6	0.1235	23.1	29.1	5	0.1632	9.1	11.3
3	0.90	1	0.0478	250.8	264.7	10	0.1184	125.0	149.9	13	0.1546	78.1	97.5
4	0.50	1	0.0095	96.7	104.7	2	0.1170	2.5	2.6	2	0.1607	1.2	0.6
4	0.75	1	0.0095	213.4	226.1	6	0.1052	30.0	37.4	6	0.1499	10.6	13.3
4	0.90	1	0.0095	303.1	318.6	9	0.1013	140.5	166.4	13	0.1431	85.0	105.6
$\gamma_0 = 0.4$													
2	0.50	2	0.1024	12.2	14.7	2	0.2013	1.7	1.4	2	0.2413	1.1	0.4
2	0.75	3	0.0955	84.9	97.1	6	0.1844	20.1	25.3	5	0.2287	8.8	10.9
2	0.90	3	0.0955	215.5	236.9	11	0.1761	117.6	142.2	13	0.2171	77.0	96.2
3	0.50	1	0.0625	30.6	34.4	2	0.1777	2.1	2.0	2	0.2261	1.2	0.5
3	0.75	1	0.0625	131.6	141.2	6	0.1614	25.2	31.6	6	0.2115	10.1	12.7
3	0.90	1	0.0625	254.2	268.2	10	0.1547	130.6	156.2	13	0.2023	83.3	103.6
4	0.50	1	0.0124	99.6	107.8	2	0.1528	2.7	2.9	2	0.2104	1.2	0.6
4	0.75	1	0.0124	217.1	229.9	6	0.1373	32.5	40.5	6	0.1961	11.8	14.8
4	0.90	1	0.0124	305.3	320.9	9	0.1321	146.3	172.8	13	0.1871	90.4	111.9
$\gamma_0 = 0.5$													
2	0.50	2	0.1253	13.2	15.8	2	0.2465	1.8	1.6	2	0.2961	1.2	0.5
2	0.75	3	0.1168	89.3	101.8	6	0.2256	22.3	28.1	6	0.2775	9.9	12.5
2	0.90	3	0.1168	220.2	241.9	12	0.2139	123.9	150.2	14	0.2647	82.9	103.6
3	0.50	1	0.0763	32.6	36.6	2	0.2171	2.3	2.2	2	0.2770	1.2	0.6
3	0.75	1	0.0763	136.6	146.5	6	0.1971	27.9	34.9	6	0.2587	11.4	14.4
3	0.90	1	0.0763	258.3	272.5	11	0.1872	137.2	164.6	13	0.2473	89.4	110.8
4	0.50	1	0.0152	103.3	111.6	3	0.1789	3.0	3.2	2	0.2573	1.3	0.8
4	0.75	1	0.0152	221.6	234.6	6	0.1672	35.8	44.4	6	0.2395	13.3	16.8
4	0.90	1	0.0152	308.0	323.7	9	0.1610	153.0	180.3	13	0.2284	96.8	119.4

Table 2. Zero-state performance. Values of H^{-*} , LCL^* , ARL_{ZS} , $SDRL_{ZS}$ for the lower-sided control charts, for different values of $n = \{5, 10, 15\}$, $p = \{2, 3, 4\}$, $\gamma_0 = \{0.1, 0.2, 0.3, 0.4, 0.5\}$, $\tau = \{0.5, 0.75, 0.9\}$ and $ARL_0 = 370.4$

p	τ	$n = 5$				$n = 10$				$n = 15$			
		H^{+*}	UCL^*	ARL_{ZS}	$SDRL_{ZS}$	H^{+*}	UCL^*	ARL_{ZS}	$SDRL_{ZS}$	H^{+*}	UCL^*	ARL_{ZS}	$SDRL_{ZS}$
$\gamma_0 = 0.1$													
2	1.10	47	0.1729	74.7	97.8	31	0.1503	44.1	57.4	24	0.1403	31.4	40.7
2	1.25	22	0.1671	17.9	22.4	12	0.1455	8.1	9.6	8	0.1359	5.1	5.8
2	1.50	10	0.1607	5.4	5.9	5	0.1408	2.4	2.2	4	0.1329	1.7	1.2
3	1.10	55	0.1569	88.5	116.0	33	0.1443	47.9	62.5	25	0.1366	33.3	43.3
3	1.25	27	0.1515	23.7	30.0	13	0.1396	9.1	10.9	9	0.1325	5.6	6.3
3	1.50	13	0.1456	7.4	8.5	6	0.1355	2.7	2.5	4	0.1290	1.8	1.4
4	1.10	71	0.1356	112.5	147.6	35	0.1378	52.6	68.6	26	0.1327	35.5	46.2
4	1.25	39	0.1310	35.8	45.9	14	0.1333	10.4	12.6	9	0.1285	6.0	7.0
4	1.50	21	0.1260	12.4	14.7	6	0.1287	3.0	3.0	4	0.1250	1.9	1.5
$\gamma_0 = 0.2$													
2	1.10	47	0.3551	76.8	100.5	31	0.3061	46.1	60.1	25	0.2850	33.1	42.9
2	1.25	22	0.3425	18.7	23.6	12	0.2958	8.6	10.3	9	0.2763	5.5	6.3
2	1.50	10	0.3285	5.7	6.4	5	0.2857	2.6	2.4	4	0.2689	1.8	1.4
3	1.10	55	0.3203	90.7	118.9	33	0.2932	50.0	65.3	26	0.2770	35.1	45.6
3	1.25	28	0.3093	24.7	31.4	13	0.2832	9.7	11.8	9	0.2680	6.0	6.9
3	1.50	14	0.2973	7.8	9.0	6	0.2744	2.9	2.7	4	0.2606	1.9	1.5
4	1.10	71	0.2747	114.8	150.7	36	0.2796	54.8	71.6	27	0.2687	37.4	48.6
4	1.25	40	0.2654	37.2	47.8	15	0.2704	11.1	13.5	10	0.2604	6.5	7.5
4	1.50	22	0.2552	13.0	15.6	6	0.2600	3.3	3.3	4	0.2521	2.0	1.7
$\gamma_0 = 0.3$													
2	1.10	48	0.5587	80.4	105.3	32	0.4740	49.5	64.6	26	0.4384	36.0	46.7
2	1.25	23	0.5372	20.3	25.6	13	0.4576	9.6	11.6	9	0.4233	6.2	7.2
2	1.50	11	0.5146	6.2	7.1	6	0.4427	2.8	2.7	4	0.4110	1.9	1.6
3	1.10	56	0.4978	94.6	124.0	34	0.4520	53.6	70.0	27	0.4250	38.1	49.6
3	1.25	29	0.4796	26.6	33.9	14	0.4362	10.8	13.2	10	0.4111	6.7	7.8
3	1.50	15	0.4604	8.6	10.0	6	0.4202	3.2	3.2	4	0.3974	2.1	1.8
4	1.10	72	0.4210	119.0	156.2	37	0.4292	58.6	76.6	27	0.4107	40.5	52.8
4	1.25	41	0.4062	39.8	51.2	16	0.4146	12.3	15.1	10	0.3970	7.2	8.6
4	1.50	23	0.3902	14.3	17.3	7	0.3994	3.6	3.8	5	0.3868	2.2	1.9
$\gamma_0 = 0.4$													
2	1.10	49	0.7993	86.0	112.7	34	0.6618	54.4	71.0	27	0.6052	40.1	52.2
2	1.25	24	0.7643	22.7	28.9	14	0.6365	11.0	13.5	10	0.5836	7.1	8.4
2	1.50	12	0.7294	7.1	8.2	6	0.6111	3.3	3.3	4	0.5625	2.2	2.0
3	1.10	57	0.6980	100.6	131.9	36	0.6268	58.8	76.9	28	0.5844	42.4	55.2
3	1.25	30	0.6697	29.6	38.0	15	0.6027	12.4	15.3	11	0.5646	7.7	9.2
3	1.50	16	0.6411	9.9	11.7	7	0.5808	3.7	3.8	5	0.5470	2.4	2.1
4	1.10	73	0.5779	125.4	164.5	38	0.5904	64.0	83.8	29	0.5632	45.0	58.7
4	1.25	43	0.5571	43.8	56.6	17	0.5692	14.1	17.6	11	0.5431	8.4	10.1
4	1.50	24	0.5332	16.3	20.0	8	0.5484	4.2	4.5	5	0.5259	2.5	2.4
$\gamma_0 = 0.5$													
2	1.10	49	1.0991	94.1	123.2	35	0.8774	60.8	79.5	28	0.7908	45.4	59.2
2	1.25	25	1.0432	26.3	33.8	15	0.8401	13.0	16.2	11	0.7607	8.5	10.2
2	1.50	13	0.9890	8.5	10.1	7	0.8057	3.9	4.1	5	0.7343	2.6	2.4
3	1.10	58	0.9307	109.3	143.2	37	0.8224	65.7	85.8	29	0.7592	48.0	62.6
3	1.25	32	0.8900	34.3	44.2	16	0.7879	14.7	18.4	12	0.7319	9.2	11.1
3	1.50	17	0.8462	11.9	14.5	8	0.7585	4.4	4.8	5	0.7037	2.8	2.7
4	1.10	73	0.7468	134.4	176.3	39	0.7671	71.3	93.3	31	0.7286	50.9	66.4
4	1.25	45	0.7195	49.9	64.7	18	0.7373	16.7	21.1	12	0.7003	10.0	12.3
4	1.50	26	0.6877	19.5	24.4	9	0.7098	5.1	5.7	6	0.6788	3.0	3.0

Table 3. Zero-state performance. Values of H^{+*} , UCL^* , ARL_{ZS} , $SDRL_{ZS}$ for the upper-sided control charts, for different values of $n = \{5, 10, 15\}$, $p = \{2, 3, 4\}$, $\gamma_0 = \{0.1, 0.2, 0.3, 0.4, 0.5\}$, $\tau = \{1.1, 1.25, 1.5\}$ and $ARL_0 = 370.4$

p	τ	$n = 5$				$n = 10$				$n = 15$			
		H^{-*}	LCL^*	ARL_{SS}	$SDRL_{SS}$	H^{-*}	LCL^*	ARL_{SS}	$SDRL_{SS}$	H^{-*}	LCL^*	ARL_{SS}	$SDRL_{SS}$
$\gamma_0 = 0.1$													
2	0.50	1	0.0303	13.5	12.3	1	0.0555	2.7	1.4	2	0.0627	2.0	0.5
2	0.75	1	0.0303	82.8	81.9	2	0.0526	21.4	20.1	2	0.0627	10.2	8.9
2	0.90	1	0.0303	211.0	210.4	3	0.0510	115.5	114.3	4	0.0604	76.5	75.1
3	0.50	1	0.0165	30.9	29.8	1	0.0495	3.1	1.9	2	0.0589	2.1	0.5
3	0.75	1	0.0165	127.2	126.3	2	0.0466	26.2	24.9	2	0.0589	11.5	10.2
3	0.90	1	0.0165	249.3	248.7	3	0.0451	127.6	126.6	4	0.0566	82.3	80.9
4	0.50	1	0.0033	97.9	97.0	1	0.0431	3.8	2.6	1	0.0575	2.2	0.7
4	0.75	1	0.0033	212.5	211.8	2	0.0403	32.9	31.7	2	0.0550	13.2	11.8
4	0.90	1	0.0033	302.1	301.5	3	0.0387	142.3	141.3	4	0.0528	88.9	87.6
$\gamma_0 = 0.2$													
2	0.50	1	0.0600	13.8	12.7	1	0.1103	2.8	1.5	2	0.1245	2.1	0.5
2	0.75	1	0.0600	84.4	83.5	2	0.1043	22.3	20.9	2	0.1245	10.7	9.4
2	0.90	1	0.0600	212.9	212.2	3	0.1011	118.1	117.0	4	0.1198	79.0	77.6
3	0.50	1	0.0327	31.6	30.5	1	0.0982	3.2	2.0	2	0.1169	2.1	0.6
3	0.75	1	0.0327	129.0	128.1	2	0.0924	27.2	25.9	2	0.1169	12.1	10.7
3	0.90	1	0.0327	250.9	250.3	3	0.0893	130.4	129.3	4	0.1124	84.9	83.5
4	0.50	1	0.0066	99.1	98.2	1	0.0853	4.0	2.7	1	0.1141	2.2	0.7
4	0.75	1	0.0066	214.1	213.4	2	0.0797	34.2	32.9	2	0.1091	13.8	12.4
4	0.90	1	0.0066	303.0	302.5	3	0.0767	145.1	144.0	4	0.1046	91.6	90.2
$\gamma_0 = 0.3$													
2	0.50	1	0.0889	14.4	13.3	1	0.1634	2.9	1.6	2	0.1846	2.1	0.5
2	0.75	1	0.0889	87.0	86.1	2	0.1545	23.7	22.4	2	0.1846	11.5	10.2
2	0.90	1	0.0889	215.9	215.2	3	0.1497	122.3	121.2	4	0.1776	82.9	81.5
3	0.50	1	0.0484	32.7	31.7	1	0.1453	3.4	2.1	2	0.1732	2.2	0.6
3	0.75	1	0.0484	131.9	131.1	2	0.1367	28.9	27.6	2	0.1732	13.0	11.7
3	0.90	1	0.0484	253.4	252.8	3	0.1320	134.6	133.6	4	0.1663	89.0	87.6
4	0.50	1	0.0098	101.2	100.3	1	0.1261	4.1	2.9	1	0.1689	2.3	0.8
4	0.75	1	0.0098	216.7	216.0	2	0.1178	36.2	34.9	2	0.1614	14.8	13.5
4	0.90	1	0.0098	304.7	304.1	3	0.1133	149.4	148.4	4	0.1547	95.8	94.5
$\gamma_0 = 0.4$													
2	0.50	1	0.1166	15.2	14.1	1	0.2143	3.0	1.7	2	0.2423	2.1	0.6
2	0.75	1	0.1166	90.6	89.7	2	0.2025	25.7	24.4	2	0.2423	12.7	11.3
2	0.90	1	0.1166	219.8	219.1	3	0.1962	127.8	126.7	4	0.2330	88.1	86.7
3	0.50	1	0.0633	34.4	33.3	1	0.1902	3.6	2.3	1	0.2372	2.2	0.8
3	0.75	1	0.0633	136.0	135.1	2	0.1788	31.3	30.0	2	0.2271	14.3	13.0
3	0.90	1	0.0633	256.8	256.2	3	0.1727	140.2	139.2	4	0.2179	94.3	93.0
4	0.50	1	0.0128	104.1	103.2	1	0.1648	4.4	3.2	1	0.2213	2.3	0.9
4	0.75	1	0.0128	220.3	219.6	2	0.1539	39.0	37.8	2	0.2114	16.3	15.0
4	0.90	1	0.0128	306.8	306.3	3	0.1480	155.1	154.1	4	0.2024	101.3	100.0
$\gamma_0 = 0.5$													
2	0.50	1	0.1427	16.3	15.2	1	0.2627	3.2	2.0	2	0.2974	2.2	0.7
2	0.75	1	0.1427	95.0	94.1	2	0.2480	28.3	27.0	2	0.2974	14.2	12.8
2	0.90	1	0.1427	224.4	223.8	3	0.2401	134.1	133.1	4	0.2857	94.2	92.8
3	0.50	1	0.0773	36.4	35.4	1	0.2327	3.8	2.6	1	0.2909	2.3	0.9
3	0.75	1	0.0773	141.0	140.2	2	0.2185	34.3	33.0	2	0.2782	16.0	14.6
3	0.90	1	0.0773	260.8	260.2	3	0.2110	146.8	145.8	4	0.2668	100.6	99.3
4	0.50	1	0.0155	107.8	106.9	1	0.2011	4.8	3.6	1	0.2709	2.4	1.0
4	0.75	1	0.0155	224.7	224.1	2	0.1876	42.6	41.3	2	0.2585	18.2	16.9
4	0.90	1	0.0155	309.5	308.9	3	0.1805	161.7	160.8	4	0.2474	107.9	106.6

Table 4. Steady-state performance. Values of H^{-*} , LCL^* , ARL_{SS} , $SDRL_{SS}$ for the lower-sided control charts, for different values of $n = \{5, 10, 15\}$, $p = \{2, 3, 4\}$, $\gamma_0 = \{0.1, 0.2, 0.3, 0.4, 0.5\}$, $\tau = \{0.5, 0.75, 0.9\}$ and $ARL_0 = 370.4$

p	τ	$n = 5$				$n = 10$				$n = 15$			
		H^{+*}	UCL^*	ARL_{SS}	$SDRL_{SS}$	H^{+*}	UCL^*	ARL_{SS}	$SDRL_{SS}$	H^{+*}	UCL^*	ARL_{SS}	$SDRL_{SS}$
$\gamma_0 = 0.1$													
2	1.10	24	0.1660	94.0	91.3	14	0.1454	58.6	56.0	11	0.1365	43.3	40.8
2	1.25	13	0.1614	27.1	24.4	7	0.1419	13.1	11.1	5	0.1334	8.7	6.9
2	1.50	7	0.1565	9.2	7.2	4	0.1390	4.4	2.8	3	0.1312	3.1	1.6
3	1.10	29	0.1501	109.4	106.8	15	0.1394	63.2	60.6	12	0.1330	45.7	43.1
3	1.25	16	0.1457	34.9	32.0	7	0.1356	14.6	12.6	5	0.1295	9.3	7.6
3	1.50	9	0.1412	12.4	10.2	4	0.1327	4.8	3.3	3	0.1273	3.3	1.8
4	1.10	45	0.1297	135.4	133.4	17	0.1332	68.7	65.9	12	0.1290	48.4	45.8
4	1.25	26	0.1258	50.9	47.4	8	0.1295	16.5	14.3	6	0.1262	10.0	8.2
4	1.50	15	0.1215	19.9	17.2	5	0.1271	5.4	3.8	3	0.1233	3.5	2.0
$\gamma_0 = 0.2$													
2	1.10	23	0.3393	96.2	93.6	14	0.2955	60.9	58.3	11	0.2766	45.3	42.9
2	1.25	13	0.3301	28.2	25.5	7	0.2882	13.9	11.9	5	0.2699	9.3	7.5
2	1.50	7	0.3195	9.7	7.7	4	0.2819	4.6	3.1	3	0.2653	3.3	1.8
3	1.10	30	0.3061	111.7	109.1	16	0.2834	65.6	62.9	12	0.2691	47.8	45.3
3	1.25	17	0.2972	36.3	33.3	8	0.2761	15.5	13.3	6	0.2633	9.9	8.0
3	1.50	10	0.2884	13.0	10.7	4	0.2684	5.1	3.5	3	0.2571	3.5	2.0
4	1.10	45	0.2623	137.8	135.9	17	0.2696	71.1	68.4	12	0.2605	50.5	48.0
4	1.25	26	0.2540	52.6	49.2	8	0.2617	17.5	15.3	6	0.2547	10.7	8.8
4	1.50	16	0.2461	20.9	18.0	5	0.2565	5.8	4.1	3	0.2485	3.7	2.2
$\gamma_0 = 0.3$													
2	1.10	24	0.5315	100.1	97.5	15	0.4568	64.8	62.2	12	0.4251	48.7	46.2
2	1.25	13	0.5143	30.2	27.5	7	0.4432	15.2	13.2	6	0.4154	10.2	8.3
2	1.50	8	0.5001	10.5	8.5	4	0.4326	5.1	3.5	3	0.4051	3.6	2.1
3	1.10	30	0.4732	115.8	113.3	16	0.4351	69.6	67.0	12	0.4113	51.3	48.8
3	1.25	17	0.4582	38.7	35.7	8	0.4231	17.0	14.8	6	0.4018	11.0	9.1
3	1.50	10	0.4435	14.2	11.9	5	0.4144	5.7	4.0	3	0.3916	3.8	2.3
4	1.10	45	0.4005	142.0	140.2	17	0.4121	75.4	72.7	13	0.3982	54.2	51.6
4	1.25	27	0.3879	55.7	52.2	9	0.4013	19.1	16.9	6	0.3877	11.8	9.9
4	1.50	16	0.3743	22.7	19.8	5	0.3908	6.4	4.7	4	0.3819	4.0	2.5
$\gamma_0 = 0.4$													
2	1.10	24	0.7527	106.0	103.4	15	0.6330	70.3	67.7	12	0.5839	53.5	51.0
2	1.25	13	0.7245	33.3	30.6	8	0.6156	17.2	15.1	6	0.5692	11.6	9.7
2	1.50	8	0.7015	11.9	9.8	4	0.5955	5.8	4.2	3	0.5536	4.0	2.5
3	1.10	30	0.6582	121.9	119.5	16	0.5991	75.4	72.8	13	0.5644	56.3	53.7
3	1.25	17	0.6348	42.4	39.5	8	0.5807	19.2	17.0	6	0.5484	12.5	10.6
3	1.50	10	0.6121	16.1	13.7	5	0.5676	6.4	4.7	4	0.5396	4.3	2.7
4	1.10	45	0.5467	148.3	146.7	17	0.5638	81.4	78.8	13	0.5429	59.4	56.8
4	1.25	27	0.5280	60.4	57.0	9	0.5476	21.6	19.3	6	0.5272	13.5	11.6
4	1.50	17	0.5103	25.5	22.5	5	0.5319	7.3	5.6	4	0.5186	4.6	3.0
$\gamma_0 = 0.5$													
2	1.10	23	1.0174	114.1	111.7	15	0.8317	77.3	74.8	12	0.7580	59.6	57.1
2	1.25	14	0.9802	37.8	35.0	8	0.8054	20.0	17.8	6	0.7363	13.6	11.6
2	1.50	8	0.9378	13.9	11.8	5	0.7851	6.7	5.0	4	0.7232	4.6	3.0
3	1.10	29	0.8658	130.5	128.3	16	0.7798	82.8	80.3	13	0.7289	62.6	60.1
3	1.25	17	0.8324	48.0	45.0	9	0.7573	22.3	20.0	7	0.7104	14.6	12.5
3	1.50	11	0.8047	18.9	16.5	5	0.7335	7.6	5.9	4	0.6930	4.9	3.4
4	1.10	44	0.7009	157.0	155.6	18	0.7293	89.2	86.6	13	0.6974	66.0	63.5
4	1.25	28	0.6776	67.3	64.0	10	0.7078	25.1	22.7	7	0.6795	15.8	13.7
4	1.50	18	0.6541	29.8	26.7	6	0.6884	8.7	6.8	4	0.6627	5.3	3.7

Table 5. Steady-state performance. Values of H^{+*} , UCL^* , ARL_{SS} , $SDRL_{SS}$ for the upper-sided control charts, for different values of $n = \{5, 10, 15\}$, $p = \{2, 3, 4\}$, $\gamma_0 = \{0.1, 0.2, 0.3, 0.4, 0.5\}$, $\tau = \{1.1, 1.25, 1.5\}$ and $ARL_0 = 370.4$

τ	$p = 2$			$p = 3$			$p = 4$		
	$n = 5$	$n = 10$	$n = 15$	$n = 5$	$n = 10$	$n = 15$	$n = 5$	$n = 10$	$n = 15$
	$\gamma_0 = 0.1$								
0.50	78	72	45	71	75	51	50	78	57
0.75	51	69	72	41	67	72	25	65	72
0.90	24	41	49	18	38	48	10	36	46
1.10	37	46	50	34	44	49	29	43	48
1.25	50	55	55	47	54	55	42	54	55
1.50	48	46	40	48	46	41	45	47	42
	$\gamma_0 = 0.2$								
0.50	78	72	46	70	76	52	49	78	58
0.75	51	69	72	41	67	72	25	65	71
0.90	24	40	48	18	38	47	10	35	46
1.10	37	45	50	33	44	49	28	43	48
1.25	50	55	56	47	54	56	42	54	56
1.50	49	47	42	48	48	43	45	48	44
	$\gamma_0 = 0.3$								
0.50	78	73	49	70	76	54	49	79	59
0.75	50	68	72	40	66	71	24	64	71
0.90	23	39	47	17	37	46	10	34	45
1.10	36	44	49	33	43	48	28	42	47
1.25	49	55	56	46	54	56	41	53	56
1.50	50	48	44	48	49	45	45	50	46
	$\gamma_0 = 0.4$								
0.50	77	74	52	69	76	57	48	79	62
0.75	49	67	71	39	65	71	23	63	70
0.90	22	38	46	17	36	45	9	33	43
1.10	35	43	48	32	42	47	27	41	46
1.25	49	55	57	46	54	56	41	53	56
1.50	51	51	47	49	51	48	46	51	49
	$\gamma_0 = 0.5$								
0.50	76	74	55	68	77	59	47	79	64
0.75	48	66	70	38	64	70	23	62	69
0.90	22	37	45	16	34	43	9	32	42
1.10	34	42	47	31	41	46	26	39	45
1.25	49	55	57	46	54	57	40	53	56
1.50	53	53	51	51	53	51	46	53	52

Table 6. Comparison vs. the Shewhart MCV control chart. Δ_E values of the Synthetic MCV control charts for different values of $p = \{2, 3, 4\}$, $n = \{5, 10, 15\}$, $\gamma_0 = \{0.1, 0.2, 0.3, 0.4, 0.5\}$, $\tau = \{0.5, 0.75, 0.9, 1.1, 1.25, 1.5\}$ and $ARL_0 = 370.4$.

Ω	p	$n = 5$	$n = 10$	$n = 15$
			$\gamma_0 = 0.1$	
(D)	2	(3, 0.0248, 96.5)	(7, 0.0475, 42.9)	(9, 0.0575, 28.3)
(I)	2	(27, 0.1687, 19.8)	(21, 0.1484, 11.9)	(19, 0.1394, 8.9)
(D)	3	(1, 0.0163, 131.3)	(7, 0.0416, 48.0)	(9, 0.0538, 30.3)
(I)	3	(30, 0.1524, 23.9)	(22, 0.1423, 12.8)	(20, 0.1357, 9.4)
(D)	4	(1, 0.0032, 203.0)	(6, 0.0360, 54.7)	(8, 0.0503, 32.7)
(I)	4	(37, 0.1306, 31.9)	(23, 0.1358, 14.0)	(20, 0.1317, 9.9)
			$\gamma_0 = 0.2$	
(D)	2	(3, 0.0492, 97.7)	(7, 0.0941, 43.9)	(9, 0.1141, 29.1)
(I)	2	(27, 0.3460, 20.4)	(21, 0.3020, 12.4)	(19, 0.2827, 9.3)
(D)	3	(1, 0.0323, 132.7)	(7, 0.0825, 49.1)	(9, 0.1066, 31.2)
(I)	3	(30, 0.3105, 24.6)	(22, 0.2889, 13.4)	(20, 0.2749, 9.8)
(D)	4	(1, 0.0064, 204.4)	(6, 0.0712, 55.9)	(9, 0.0990, 33.6)
(I)	4	(37, 0.2641, 32.8)	(23, 0.2750, 14.6)	(20, 0.2663, 10.3)
			$\gamma_0 = 0.3$	
(D)	2	(3, 0.0729, 99.7)	(7, 0.1392, 45.5)	(9, 0.1689, 30.4)
(I)	2	(27, 0.5420, 21.5)	(21, 0.4664, 13.2)	(19, 0.4340, 10.0)
(D)	3	(1, 0.0478, 134.9)	(7, 0.1219, 50.9)	(9, 0.1578, 32.6)
(I)	3	(30, 0.4805, 25.9)	(22, 0.4444, 14.3)	(19, 0.4202, 10.5)
(D)	4	(1, 0.0095, 206.6)	(6, 0.1052, 57.8)	(9, 0.1463, 35.1)
(I)	4	(37, 0.4034, 34.5)	(23, 0.4210, 15.5)	(20, 0.4067, 11.1)
			$\gamma_0 = 0.4$	
(D)	2	(3, 0.0955, 102.5)	(8, 0.1804, 47.7)	(9, 0.2214, 32.2)
(I)	2	(26, 0.7682, 23.2)	(21, 0.6482, 14.5)	(19, 0.5977, 11.0)
(D)	3	(1, 0.0625, 138.0)	(7, 0.1593, 53.2)	(9, 0.2066, 34.4)
(I)	3	(29, 0.6682, 27.9)	(21, 0.6121, 15.6)	(19, 0.5763, 11.5)
(D)	4	(1, 0.0124, 209.6)	(6, 0.1373, 60.4)	(9, 0.1913, 37.0)
(I)	4	(37, 0.5510, 37.2)	(22, 0.5761, 17.0)	(20, 0.5556, 12.2)
			$\gamma_0 = 0.5$	
(D)	2	(3, 0.1168, 105.8)	(8, 0.2206, 50.3)	(9, 0.2712, 34.3)
(I)	2	(25, 1.0432, 25.7)	(20, 0.8529, 16.1)	(19, 0.7785, 12.3)
(D)	3	(1, 0.0763, 141.9)	(7, 0.1945, 56.1)	(9, 0.2526, 36.7)
(I)	3	(29, 0.8832, 31.0)	(21, 0.7992, 17.4)	(19, 0.7463, 12.9)
(D)	4	(1, 0.0152, 213.5)	(6, 0.1672, 63.5)	(9, 0.2336, 39.4)
(I)	4	(37, 0.7082, 41.2)	(22, 0.7452, 19.0)	(19, 0.7142, 13.6)

Table 7. Zero-state performance. Optimal couples (H^{*-}, LCL^*) for $\Omega = [0.5, 1)$ and (H^{+*}, UCL^*) for $\Omega = (1, 2]$ (two first values of each column) and out-of-control $EARL$ (last values of each column) with unknown shift size for $n = \{5, 10, 15\}$, $p = \{2, 3, 4\}$, $\gamma_0 = \{0.1, 0.2, 0.3, 0.4, 0.5\}$ and $ARL_0 = 370.4$. (D), decreasing case; (I), increasing case; EARL, expected average run length.

Ω	p	$n = 5$	$n = 10$	$n = 15$
		$\gamma_0 = 0.1$		
(D)	2	(1, 0.0303, 100.9)	(3, 0.0510, 47.9)	(3, 0.0613, 32.6)
(I)	2	(15, 0.1625, 25.9)	(11, 0.1442, 15.9)	(10, 0.1362, 12.1)
(D)	3	(1, 0.0165, 135.0)	(2, 0.0466, 53.1)	(3, 0.0576, 34.8)
(I)	3	(17, 0.1462, 31.1)	(11, 0.1379, 17.1)	(10, 0.1323, 12.7)
(D)	4	(1, 0.0033, 206.2)	(2, 0.0403, 59.8)	(3, 0.0537, 37.3)
(I)	4	(25, 0.1255, 41.3)	(12, 0.1316, 18.5)	(10, 0.1283, 13.3)
		$\gamma_0 = 0.2$		
(D)	2	(1, 0.0600, 102.1)	(3, 0.1011, 48.9)	(3, 0.1217, 33.5)
(I)	2	(15, 0.3325, 26.7)	(11, 0.2930, 16.5)	(9, 0.2750, 12.6)
(D)	3	(1, 0.0327, 136.4)	(2, 0.0924, 54.2)	(3, 0.1142, 35.7)
(I)	3	(17, 0.2972, 32.0)	(11, 0.2795, 17.7)	(10, 0.2676, 13.2)
(D)	4	(1, 0.0066, 207.5)	(2, 0.0797, 61.0)	(3, 0.1064, 38.3)
(I)	4	(25, 0.2534, 42.5)	(12, 0.2660, 19.2)	(10, 0.2590, 13.9)
		$\gamma_0 = 0.3$		
(D)	2	(1, 0.0889, 104.2)	(3, 0.1497, 50.7)	(3, 0.1804, 35.0)
(I)	2	(14, 0.5165, 28.0)	(10, 0.4497, 17.5)	(9, 0.4211, 13.5)
(D)	3	(1, 0.0484, 138.7)	(2, 0.1367, 56.1)	(3, 0.1691, 37.2)
(I)	3	(17, 0.4582, 33.6)	(11, 0.4287, 18.9)	(9, 0.4074, 14.1)
(D)	4	(1, 0.0098, 209.7)	(2, 0.1178, 63.0)	(3, 0.1574, 39.8)
(I)	4	(25, 0.3859, 44.6)	(11, 0.4048, 20.4)	(10, 0.3948, 14.8)
		$\gamma_0 = 0.4$		
(D)	2	(1, 0.1166, 106.9)	(3, 0.1962, 52.9)	(3, 0.2368, 36.9)
(I)	2	(14, 0.7280, 30.1)	(10, 0.6219, 19.1)	(9, 0.5779, 14.7)
(D)	3	(1, 0.0633, 141.8)	(2, 0.1788, 58.6)	(3, 0.2216, 39.2)
(I)	3	(17, 0.6348, 36.1)	(11, 0.5893, 20.5)	(9, 0.5569, 15.4)
(D)	4	(1, 0.0128, 212.7)	(2, 0.1539, 65.7)	(3, 0.2060, 41.9)
(I)	4	(24, 0.5235, 47.8)	(11, 0.5528, 22.2)	(9, 0.5356, 16.2)
		$\gamma_0 = 0.5$		
(D)	2	(1, 0.1427, 110.3)	(3, 0.2401, 55.7)	(3, 0.2904, 39.1)
(I)	2	(13, 0.9746, 33.1)	(10, 0.8149, 21.1)	(9, 0.7491, 16.2)
(D)	3	(1, 0.0773, 145.6)	(2, 0.2185, 61.5)	(3, 0.2714, 41.6)
(I)	3	(16, 0.8286, 39.8)	(10, 0.7615, 22.7)	(9, 0.7180, 17.0)
(D)	4	(1, 0.0155, 216.5)	(2, 0.1876, 69.0)	(3, 0.2519, 44.5)
(I)	4	(23, 0.6672, 52.7)	(11, 0.7114, 24.7)	(9, 0.6869, 17.9)

Table 8. Steady-state performance. Optimal couples (H^{*-} , LCL^*) for $\Omega = [0.5, 1)$ and (H^{*+} , UCL^*) for $\Omega = (1, 2]$ (two first values of each column) and out-of-control $EARL$ (last values of each column) with unknown shift size for $n = \{5, 10, 15\}$, $p = \{2, 3, 4\}$, $\gamma_0 = \{0.1, 0.2, 0.3, 0.4, 0.5\}$ and $ARL_0 = 370.4$. (D), decreasing case; (I), increasing case; EARL, expected average run length.

Ω	$p = 2$			$p = 3$			$p = 4$		
	$n = 5$	$n = 10$	$n = 15$	$n = 5$	$n = 10$	$n = 15$	$n = 5$	$n = 10$	$n = 15$
	$\gamma_0 = 0.1$								
(D)	40	45	46	35	44	46	24	44	46
(I)	36	40	42	34	39	41	32	39	41
	$\gamma_0 = 0.2$								
(D)	39	44	46	35	44	46	24	43	45
(I)	36	40	42	34	39	41	32	39	41
	$\gamma_0 = 0.3$								
(D)	39	44	45	35	43	45	24	43	45
(I)	36	40	41	35	39	41	32	39	41
	$\gamma_0 = 0.4$								
(D)	38	43	45	34	43	45	23	42	44
(I)	36	40	41	35	39	41	32	39	41
	$\gamma_0 = 0.5$								
(D)	38	43	44	33	42	44	23	42	44
(I)	37	40	42	36	40	41	33	39	41

Table 9. Comparison vs. the Shewhart MCV control chart. Δ_E values of the Synthetic MCV control charts with unknown shift for different values of $p = \{2, 3, 4\}$, $n = \{5, 10, 15\}$, $\gamma_0 = \{0.1, 0.2, 0.3, 0.4, 0.5\}$ and $ARL_0 = 370.4$.

p	τ	n = 5				n = 10			
		zero-state		steady-state		zero-state		steady-state	
		Syn MCV	RS MCV	Syn MCV	RS MCV	Syn MCV	RS MCV	Syn MCV	RS MCV
$\gamma_0 = 0.1$									
2	0.50	10.6	6.4	13.5	4.3	1.5	2.6	2.7	2.0
	0.75	77.2	28.9	82.8	24.7	16.3	10.6	21.4	7.8
	0.90	206.3	122.1	210.8	118.2	105.3	61.0	115.4	57.0
	1.10	74.7	88.3	94.0	86.1	44.1	48.9	58.6	47.3
	1.25	17.9	23.8	27.1	22.0	8.1	10.5	13.1	9.0
	1.50	5.4	7.8	9.2	6.8	2.4	3.6	4.4	3.0
3	0.50	27.3	9.6	30.9	6.3	1.8	3.0	3.1	2.2
	0.75	122.6	43.7	127.0	39.3	20.6	12.1	26.2	9.0
	0.90	246.3	153.8	249.1	150.4	117.9	68.1	127.5	64.0
	1.10	88.4	107.1	109.3	105.0	47.9	53.7	63.2	51.5
	1.25	23.7	32.3	34.9	30.7	9.1	11.8	14.6	10.2
	1.50	7.4	10.8	12.4	9.8	2.7	4.0	4.8	3.3
$\gamma_0 = 0.3$									
2	0.50	11.4	6.7	14.4	4.4	1.6	2.8	2.9	2.1
	0.75	81.3	30.7	87.0	26.5	18.3	11.6	23.7	8.5
	0.90	211.3	127.2	215.6	123.5	112.1	66.1	122.2	62.0
	1.10	80.4	94.4	100.0	92.2	49.4	54.7	64.7	52.5
	1.25	20.2	26.6	30.2	24.8	9.6	12.1	15.2	10.6
	1.50	6.2	8.9	10.5	7.8	2.8	4.2	5.1	3.5
3	0.50	29.0	10.0	32.7	6.6	1.9	3.1	3.4	2.3
	0.75	127.4	46.4	131.8	42.1	23.1	13.1	28.9	9.9
	0.90	250.5	159.3	253.2	156.0	124.9	73.4	134.5	69.3
	1.10	94.5	113.3	115.7	112.1	53.6	60.1	69.6	57.9
	1.25	26.6	35.9	38.6	34.4	10.8	13.7	17.0	12.0
	1.50	8.6	12.5	14.2	11.4	3.2	4.7	5.7	3.9
$\gamma_0 = 0.5$									
2	0.50	13.2	7.2	16.3	4.83	1.8	3.0	3.2	2.2
	0.75	89.2	34.7	94.9	30.4	22.2	13.3	28.2	10.1
	0.90	220.0	137.3	224.2	133.6	123.8	75.5	134.0	71.4
	1.10	94.0	108.2	114.0	106.9	60.8	66.6	77.2	64.4
	1.25	26.3	33.5	37.8	31.8	13.0	15.9	20.0	14.1
	1.50	8.5	11.9	13.9	10.6	3.9	5.5	6.7	4.6
3	0.50	32.6	10.7	36.4	7.3	2.3	3.4	3.8	2.5
	0.75	136.5	52.1	140.8	47.7	27.8	15.2	34.3	11.9
	0.90	258.0	169.7	260.6	166.5	137.1	83.4	146.6	79.3
	1.10	109.2	127.7	130.4	126.5	65.6	72.0	82.7	70.5
	1.25	34.3	44.9	47.9	43.2	14.7	17.8	22.3	16.1
	1.50	11.9	17.0	18.9	15.6	4.4	6.2	7.6	5.2

Table 10. Comparison with the run sum control charts, for different values of $n = \{5, 10\}$, $p = \{2, 3\}$, $\gamma_0 = \{0.1, 0.2, 0.3\}$, $\tau = \{0.5, 0.75, 0.9, 1.10, 1.25, 1.50\}$ and $ARL_0 = 370$.

p	τ	n = 5				n = 10			
		Syn MCV	VSSI MCV	VSI MCV	VSS MCV	Syn MCV	VSSI MCV	VSI MCV	VSS MCV
		$\gamma_0 = 0.1$							
2	1.25	27.08	16.99	31.48	19.29	13.10	5.79	11.84	8.80
	1.50	9.19	4.19	7.32	5.33	4.36	1.66	1.74	2.70
3	1.25	34.92	26.37	41.82	28.28	14.61	6.79	13.98	9.83
	1.50	12.40	6.28	11.82	7.29	4.82	1.86	1.96	2.92
$\gamma_0 = 0.3$									
2	1.25	30.18	20.88	35.69	23.54	15.24	7.30	14.49	10.95
	1.50	10.53	4.94	9.25	6.08	5.08	1.93	2.03	3.08
3	1.25	38.67	31.93	46.81	34.06	16.97	8.64	17.01	12.29
	1.50	14.20	7.55	14.42	8.55	5.65	2.21	2.37	3.36
$\gamma_0 = 0.5$									
2	1.25	37.77	30.62	46.94	34.02	19.98	11.18	20.74	16.14
	1.50	13.93	6.79	14.81	8.09	6.74	2.60	4.57	4.05
3	1.25	47.97	45.14	60.17	47.68	22.27	13.33	24.16	18.24
	1.50	18.92	10.81	21.90	11.99	7.58	3.00	5.79	4.48

Table 11. Comparison with the other adaptive control charts proposed in [29] under the steady-state condition, for different values of $n = \{5, 10\}$, $p = \{2, 3\}$, $\gamma_0 = \{0.1, 0.2, 0.3\}$, $ARL_0 = 370.4$ and upper shifts $\tau = \{1.25, 1.50\}$.